Supplementary material: Depth profile analysis of Deep Level Defects in 4H−SiC introduced by radiation
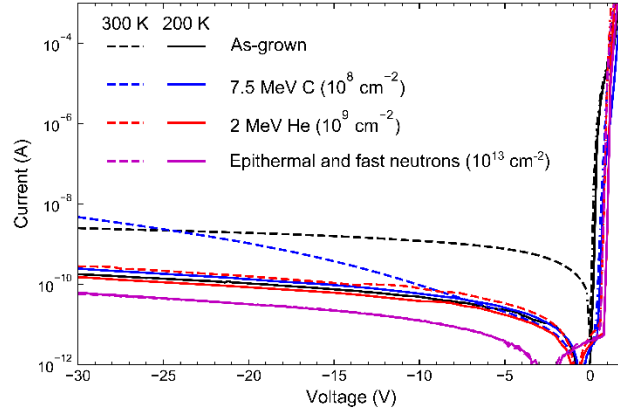

Figure S1. Current−voltage characteristics of SBDs implanted with 7.5 MeV C (10^8 cm^{-2}) and 2 MeV He (10^9 cm^{-2}) ions, and neutron irradiated (10^{13} cm^{-2}) SBD at temperatures of 200 K and 300 K.

Figure S1 shows current−voltage characteristics of the SBD at temperatures of 200 K and 300 K. The reverse current is less than 10 nA in the whole voltage range down to −30 V, clearly showing rectifying characteristics.
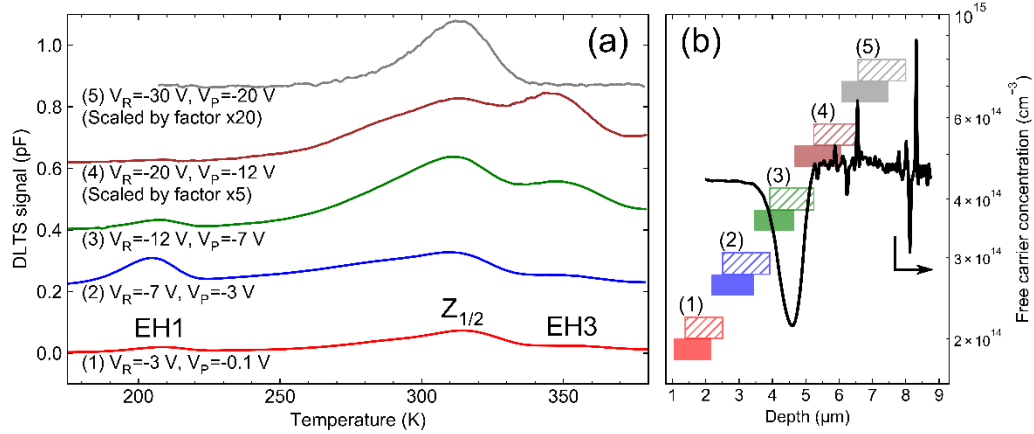

Figure S2. (**a**) DLTS spectra of 2 MeV He (10^9 cm^{-2}) ion implanted n-type 4H-SiC SBD. Different voltage settings, reverse bias V_R and pulse bias V_P, are used to probe different depth ranges (as seen in (**b**)). The rate window and pulse width t_P are 50 s^{-1} and 10 ms. The spectra are shifted vertically for clarity. (**b**) Schematic illustration of the depth regions contributing to the DLTS signal of EH1 at 210 K (hatched rectangles) and EH3 at 350 K (solid rectangles) for the used voltage in the DLTS measurements (as seen in (**a**)). The lambda effect was taken into account. The depth ranges are compared with free carrier concentration (black line) determined from C−V characteristic at 200 K (as in Figure **Error! Reference source not found.**2), which exhibits a minimum due to introduced acceptor deep levels.
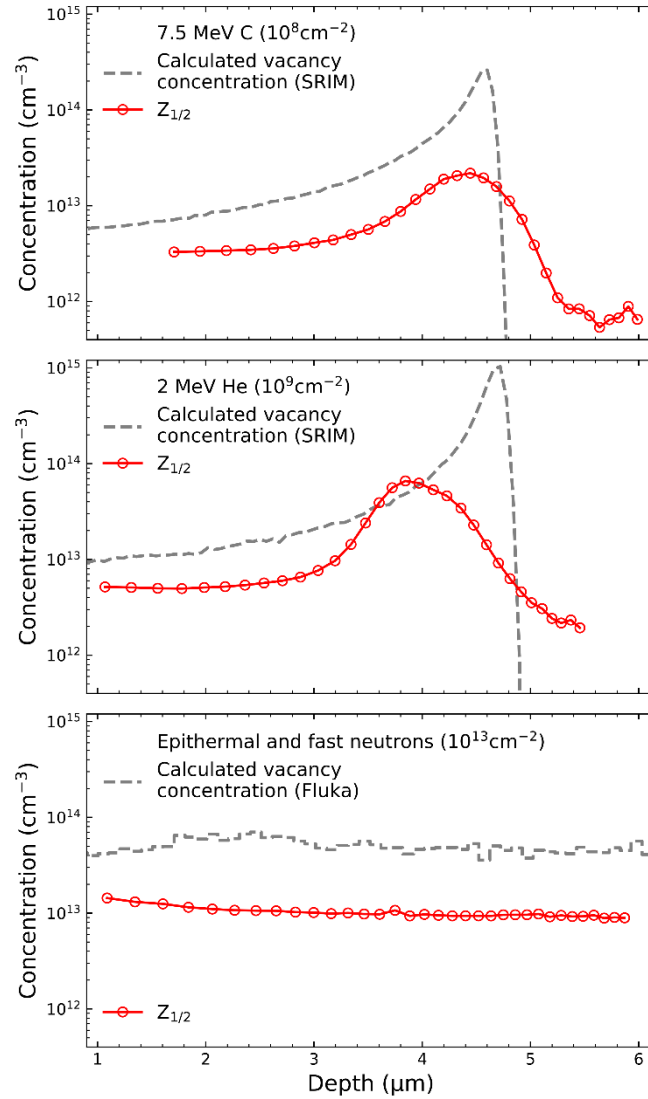
Figure S3. Depth concentration profiles for $Z_{1/2}$ deep level and total introduced vacancies calculated by SRIM and Fluka software [1,2]. The lambda effect was taken into account [3]. Depth profiling measurements were carried out at the temperature of 315 K.

Figure S2 shows a series of DLTS measurements carried out on He (10^9 cm^{-2}) ion implanted sample with different voltage settings selected for probing deep levels in adjacent depth ranges. A higher concentration of EH3 deep level compared to EH1 deep level is observed at the ion depth range, while only $Z_{1/2}$ deep level is observed in the region beyond the ion depth range (similarly as in Figure 5).

Figure S5Figure S3 shows the depth concentration profiles of $Z_{1/2}$ deep level, supplementing depth profiles shown in Figure 6. The Lambda lengths used in equation (1) are calculated by numerical integration of Poisson's equation using the following expression [3]:

$$\frac{E_T - E_F}{q} = \frac{q}{\varepsilon_0 \varepsilon_r} \int_{L-\lambda}^{L} N_D(x)(x - (L - \lambda))\, dx$$

Where L is space charge region width at applied reverse voltage, N_D the free carrier concentration measured at the temperature of 200 K, E_F Fermi level, and E_T the activation energy of a deep level.
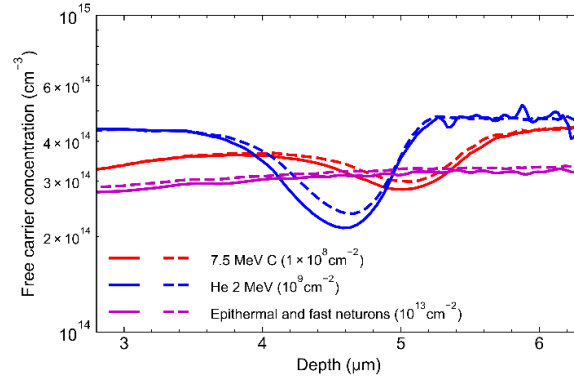

Figure S4. Increase in free carrier concentration after annealing at the temperature of 450 K. Solid and dashed lines show free carrier concentration profiles measured before and after annealing at the temperature of 450 K, respectively. The profiles are calculated using C−V measurements at a temperature of 200 K.
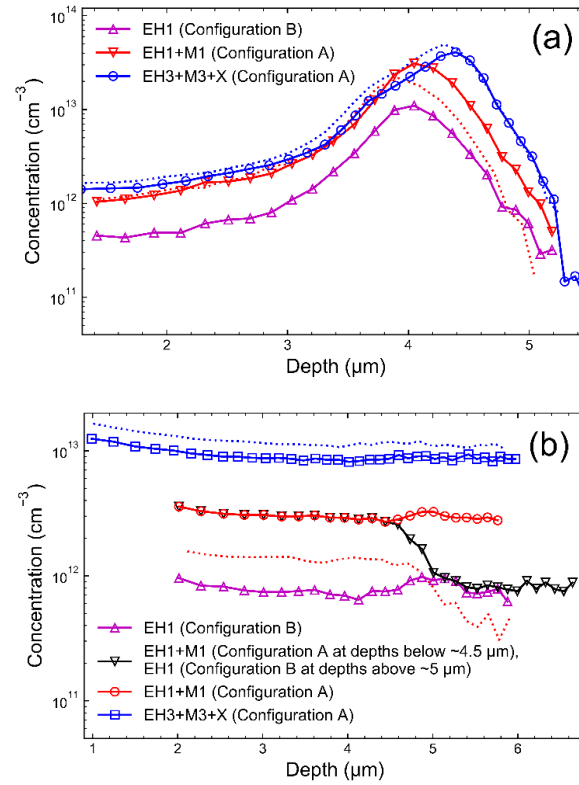

Figure S5. EH1, EH1 and M1, EH3 and M3 depth concentration profiles in (**a**) 2 MeV He (10^9 cm^{-2}) ion implanted and (**b**) neutron (10^{13} cm^{-2}) irradiated SBD. The shown EH1+M1 concentration profile (Configuration A) was measured after cooling SBD from 340 K down to 210 K under −30V bias, while EH1 profile was measured after cooling down SBD from 450 K without bias. The black curve in (**b**) shows depth concentration profile measured after cooling SBD from 340 K down to 210 K under −10V bias. Depth profiles

measured before 450 K annealing (as seen in Figure 6) are shown with dotted lines. The contribution of an additional deep level defect involving interstitials is labeled as X.

In He (10^9 cm^{-2}) ion implanted SBD (Figure S5a), depth of EH3 + M3 + X profile maximum (4.39 ± 0.1 μm) showed a shift towards greater depths compared to EH1+M1 and EH1 profile maximums at (4.05 ± 0.2 μm). Homogenous EH1, EH1 + M1, and EH3 + M3 + X concentration profiles are observed in neutron (10^{13} cm^{-2}) irradiated SBD (Figure S5b). When the SBD is cooled down from 340 K to 210 K with reverse bias −10 V before profile measurements, regions with M-center in configurations A and B are present in the observed depth range (black line in Figure S5b). The depth between those two regions is determined by the lambda length and space charge region width at −10 V reverse bias in the temperature range 290 K–340 K.

Concentration depth profiles and capture kinetics of M−center shown in Figure S5b and Figure S6 are consistent with results previously reported by Martin et al. and Nielsen et al. [4,5], displaying equivalent observations in cases of neutron irradiation and 1–2.5 MeV proton ion implantation.
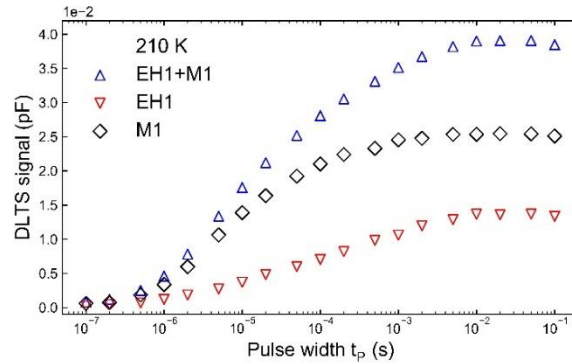

Figure S6. Pulse width dependence of EH1 and EH1+M1 DLTS signal amplitudes in neutron (10^{13} cm^{-2}) irradiated SBD. DLTS signal amplitude of M1 deep level is determined by subtracting EH1+M1 and EH1 DLTS signals. Measurements are carried out at a temperature of 210 K using 50 1/s emission rate window. Reverse and pulse voltages were −10 V and −0.1 V, respectively.

References

1. Battistoni G, Cerutti F, Fassò A, Ferrari A, Muraro S, Ranft J, Roesler S, Sala PR (2007) The FLUKA code: Description and benchmarking. AIP Conf Proc 896:31–49 . doi: 10.1063/1.2720455

2. Ziegler JF, Ziegler MD, Biersack JP (2010) SRIM − The stopping and range of ions in matter (2010). Nucl Instruments Methods Phys Res Sect B Beam Interact with Mater Atoms 268:1818–1823 . doi: 10.1016/j.nimb.2010.02.091

3. Zohta Y, Watanabe MO (1982) On the determination of the spatial distribution of deep centers in semiconducting thin films from capacitance transient spectroscopy. J Appl Phys 53:1809–1811 . doi: 10.1063/1.330683

4. Martin DM, Kortegaard Nielsen H, Lévêque P, Hallén A, Alfieri G, Svensson BG (2004) Bistable defect in mega−electron−volt proton implanted 4H silicon carbide. Appl Phys Lett 84:1704–1706 . doi: 10.1063/1.1651656

5. Nielsen HK, Hallén A, Svensson BG (2005) Capacitance transient study of the metastable M center in n −type 4H−SiC. Phys Rev B − Condens Matter Mater Phys 72:085208 . doi: 10.1103/PhysRevB.72.085208